Adv. Sci. Res., 22, 13–18, 2025
https://doi.org/10.5194/asr-22-13-2025

Advances in Science & Research
Open Access Proceedings

The influence of absorbing aerosols on the morning PBL growth dynamic in the EDMF-AERO modeling framework

Grzegorz M. Florczyk and Krzysztof M. Markowicz

Institute of Geophysics, Faculty of Warsaw, University of Warsaw, Warsaw, Poland

Correspondence: Grzegorz M. Florczyk (gflorczyk@fuw.edu.pl)

Received: 28 February 2025 – Revised: 25 May 2025 – Accepted: 28 May 2025 – Published: 17 July 2025

Abstract. Using the novel PBL evolution model EDMF-AERO and the dataset collected during a measurement campaign at the Swider Geophysical Observatory in 2014, we studied morning PBL dynamics under high pollution. We tuned the model to the data and reached good accuracy in PBLH estimation (3 % deviation) and sufficient accuracy in the average potential temperature of PBL $\overline{\theta_{\mathrm{PBL}}}$ estimation (RMSE = 2.7 K). The study focused on the Aerosol-PBL Interactions (API). In particular, we examined the influence of absorbing aerosol on the morning dynamics of PBL growth. Although no significant change in the height of the developed PBL was found, a nonzero convection onset delay was detected alongside the rapid formation of thermals. We also evaluated which one of the API component effects ("Surface cooling" or "Aerosol heating") is dominant in terms of influence on $\overline{\theta_{\mathrm{PBL}}}$ and PBLH. The "Aerosol heating" component impacts $\overline{\theta_{\mathrm{PBL}}}$ variability around two times stronger than the "Surface cooling" component. In terms of PBLH, the two components are approximately equal in strength and cancel each other out, yielding no change in PBLH under heavy pollution compared to the clear-sky case.

1 Introduction

The Earth's climate system is critically important from a scientific perspective, as it is a system that can be described as chaotic and challenging to model mathematically. Many of the mathematical equations employed to understand this system are analytically unsolvable, necessitating the use of numerical methods (Stull, 1988). The more complex the interactions, the more attention and caution are required in constructing numerical models. A prime example of such interactions in the climate system is the group of mechanisms involving radiative effects from atmospheric aerosols and the dynamics of the lowest layer of the troposphere, known as the Planetary Boundary Layer (PBL). This group includes numerous well-documented aerosol-cloud interactions (aci), such as the Twomey (1959) and Albrecht (1989) effects, as well as aerosol-radiation interactions (ari), such as the blocking of energy reaching the Earth's surface by absorbing aerosols, or the heating of higher atmospheric layers that enhances thermal inversion. These two groups form the primary pillars of the combined aerosol-PBL interaction (API).

The difficulty with assessing the influence of aerosols on PBL growth dynamics is best exemplified by its dependence on aerosol vertical distribution. Research conducted by Li et al. (2017), Huang et al. (2018), Lisok et al. (2018), Luo et al. (2022), Su et al. (2020, 2022), Ma et al. (2022) has shown various ways aerosols can influence the PBL. Of particular significance is the feedback mechanism linking the concentration of absorbing aerosols to the planetary boundary layer height (PBLH), as highlighted in several studies (Barbaro et al., 2014; Miao et al., 2019; Ma et al., 2020, 2022). The diversity of observed outcomes has led to the classification of APIs into distinct categories based on the vertical distribution of aerosols. Among these, the "stove" and "dome" effects have emerged as two primary conceptual models. These effects have been further investigated using the EDMF-AERO framework in Florczyk et al. (2025).

Despite being a significant health issue, days with intense pollution in PBL offer a valuable opportunity to study API (Aerosol-PBL Interactions) mechanisms under controlled conditions. Researchers studying this topic often look for quality in situ profiles collected during such episodes to ini-

Published by Copernicus Publications.

tialize numerical models with. After sufficient tuning, these models can be used to conduct more simulations and to study how the morning PBL dynamics would change with negligible or doubled aerosol concentration. Such studies are invaluable from a scientific standpoint, providing quantitative and qualitative insights into the strength of the API components. Subsequently, given that numerical models are built modularly, we can study API effects individually to identify a dominant one.

A model developed by Florczyk et al. (2025) at the University of Warsaw and NASA Jet Propulsion Laboratory, known as EDMF-AERO, addresses these needs. This single-column model is based on the Eddy-Diffusivity Mass Flux framework (Siebesma and Teixeira, 2000; Soares et al., 2004; Siebesma et al., 2007; Han et al., 2016) and the Ed4-LaRC-Fu-Liou Radiation Transfer Model (RTM) developed at NASA Langley Center based on the parametrization by Fu and Liou (1992). Notably, EDMF-AERO was validated against in-situ measurements and showed satisfactory agreement and enables the user to turn off API component effects to study PBL evolution with just one of them active. In this study, we used EDMF-AERO to analyze the morning growth dynamics of PBL with high absorbing aerosol concentration. We focused on two effect components called "Atmospheric heating" (additional heating of the air due to the presence of absorbing aerosols) and "Surface cooling" (decrease of surface temperature due to absorbing aerosols blocking radiation from reaching it). These effect components were thoroughly explained in recent studies addressing the topic of API (Miao et al., 2019; Ma et al., 2020).

2 Methods

2.1 Measurements

We used archival data from the PolandAOD network (Markowicz et al., 2021). In 2014, on 28 and 29 October, a measurement campaign was conducted in the Swider Geophysical Observatory (52.11° N, 21.23° E, 94 m a.s.l.), near Warsaw (Chiliński et al., 2018). During these 2 d, the following measurements were performed:

- Profiles of the backscattering coefficient β were collected using a Vaisala CL31 ceilometer (Sokół et al., 2014). These profiles were additionally corrected for overlap almost to the ground level using the internal algorithm. After verification, Chiliński et al. (2018) assumed that the usable profiles were 60–100 m above ground level.

- The Photoacoustic Extinctiometer (PAX) operating at $\lambda = 870$ nm was used to measure the optical properties of aerosols such as the scattering coefficient $\sigma_s(z)$, the absorption coefficient $\sigma_a(z)$, the single scattering albedo ω and the eBC concentration (Nakayama et al., 2015).

- Aerosol concentration in terms of the Black Carbon Equivalent (eBC) and thermodynamical profiles were collected using a measurement platform consisting of a Vaisala RS92-SGP radiosonde (Nash et al., 2010) and Aethlabs micro-aethalometer AE-51 (Ferrero et al., 2014; Chilinski et al., 2016) mounted on a small unmanned aerial system (sUAS) Versa X6sci hexacopter manufactured by Versadrones

Although Chiliński et al. (2018) focused on the potential of combining lidar and sUAS measurements to fill gaps and create a comprehensive atmospheric profile, their study also produced a valuable dataset interesting to analyze using EDMF-AERO. During the night 28/29, high aerosol concentrations (eBC $=\sim 54\,\mu m^3$ near the surface) moved over the Swider Geophysical Observatory. The pollution remained close to the ground, up to a height of approximately 70 m, throughout the night. With sunrise, the morning evolution of the PBL began. The measurements were repeated at 10:30 LT.

2.2 Data

Despite the rich dataset, the sUAS only reached an altitude of approximately 400 m. EDMF-AERO requires profiles up to an altitude of 4 km, while the RTM is up to 100 km. We extended profiles by combining RS92-SGP measurements with soundings from WMO #12374 Legionowo station (52.40° N, 20.95° E, 73 m a.s.l.) and the "jlms.lay" file (standard atmosphere up to 100 km). The exception is the wind profile, which was taken entirely from Legionowo. The Legionowo station is ~ 50 km away from the Swider site, which is close enough to represent similar meteorological and aerosol conditions. Moreover, both sites are located in the Warsaw suburbs (the Polish capital), are surrounded by forest, and have the same topography and surface type (grassland). Overall, their characteristic are very similar.

To obtain additional information on the temporal evolution of PBLH, we used the method of extracting PBLH from the CL31 β profile. Caicedo et al. (2017) compared three methods used to derive PBLH from CL31 aerosol β profile against radiosonde measurements: (1) Vaisala Corp. BL Matlab v3.7 gradient algorithm, (2) K-means cluster analysis (Toledo et al., 2014), and (3) Covariance wavelet transform with Haar wavelet (Brooks, 2003). The Haar wavelet method proved to be the most reliable, so for this study, we used a Python library prepared by the Spectroscopy and Remote Sensing (EPR) Group at UNAM Mexico, using the Red Universitaria de Observatorios Atmosfericos (RUOA) instruments that allow for the extraction of PBLH using this method (Garcia-Franco and Stremme, 2018; García-Franco et al., 2018; Grabon et al., 2010). Besides PBLH, the algorithm also returns the lower and upper bounds of the estimate. It is worth noting that despite applied corrections, the CL31 still cannot reliably measure backscatter below 60–100 m. In such cases, it is useful to know the PBLH a priori. In this

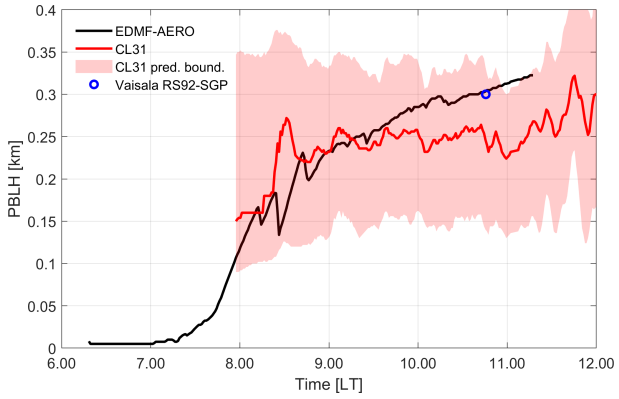

Figure 1. The comparative plot of the variability of PBLH was determined with Radiosonde Vaisala RS92-SGP (blue marker), EDMF-AERO (black line), and CL31 (red line). The bright red area indicates the uncertainty range of PBLH determined from CL31 data.

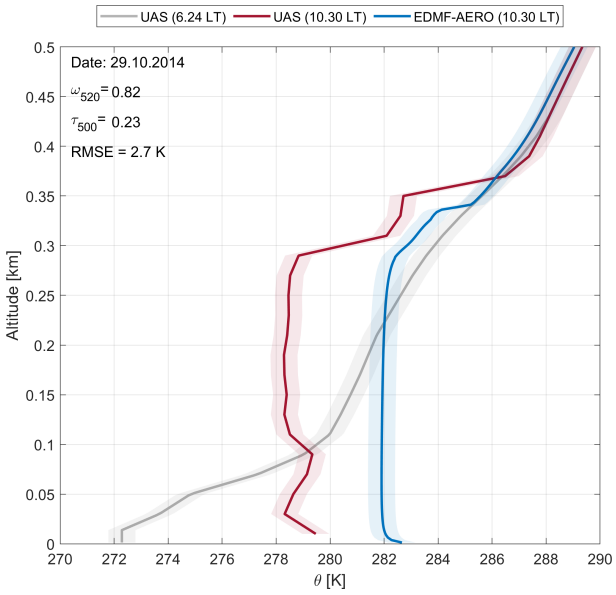

Figure 2. Comparison of θ profiles predicted by EDMF-AERO (blue line) with data collected with the UAS measurement platform (red line). The gray line indicates the initial profile. Areas of analogous colors denote uncertainty ranges.

case, RS92-SGP returns PBLH of around 70 m, which is a detection limit of the CL31. Given that the profiling was done in the morning hours and we do not observe distinct thermal inversion in θ profile (see Fig. 2), the algorithm probably fails to find the PBLH due to the boundary layer still being in the stable regime. Given that information, we assumed an initial PBLH = 0. PBLH temporal variability was visualized in Fig. 1 together with EDMF-AERO prediction and in situ measurement.

2.3 Surface heat fluxes

Together with initial thermodynamic profiles, the EDMF-AERO was supplied with the surface heat fluxes parametrization prepared analogously to Florczyk et al. (2025) and defined as in Eq. (1). We used data from the SolarAOT station for October 2022. The site is located in the southeast part of Poland (49.878° N, 21.861° E, 443 m a.s.l.) on a small hill in a predominantly rural area. Despite the large distance, it provides a representative dataset regarding a rural grassland near a small city. Unfortunately, during this period, the latent heat measurements returned erroneous values, thus, we reused values from Florczyk et al. (2025).

$$Q_S = \frac{1}{\rho c_p}[0.141 \cdot F_{SW}^{\downarrow} - 22.1],$$
$$Q_L = \frac{1}{\rho L_v}[0.129 \cdot F_{SW}^{\downarrow} + 21.1] \quad (1)$$

Where Q_S is the sensible heat flux, Q_L is the latent heat flux, $F_{SW}^{\downarrow}$ is the downward SW radiation flux, ρ is the density of air, L_v is the latent heat of vaporization (2.501×10^6 J kg^{-1}), c_p is the specific heat capacity of air at constant pressure (1005.7 J kg^{-1} K^{-1}).

3 Model validation

As can be seen in the Fig. 2, although EDMF-AERO tends to overestimate the potential temperature (RMSE = 2.7 K), it is exceptionally good in predicting PBLH, which was estimated at 0.30 km, or ∼ 10 m (3 %) more than the measured PBLH. The simulated $\overline{\theta}$ is ∼ 3 K higher than the actual.

In the next step, we focused on the dynamics of the PBLH growth just after sunrise. Figure 1 shows a comparison of the PBLH determined with the CL31 and the EDMF-AERO prediction. In this study, we are interested in the general study of API rather than the exact replication of the atmospheric system in Swider on that day. Notably, there is a high level of uncertainty in the PBLH assessment, but EDMF-AERO shows excellent agreement with radiosonde measurement (see Fig. 1). The authors claim that these results, complemented by EDMF-AERO validation from Florczyk et al. (2025), are sufficient to try to draw further conclusions about PBL dynamics under polluted conditions.

4 Results

Firstly, we simulated the PBLH growth dynamics with higher and lower aerosol optical depths τ_{500} (500 means measured at wavelengths $\lambda = 500$ nm). As can be seen in Fig. 3, the change in absorbing aerosol concentration did not significantly affect the PBLH at the end of the simulation. All of the additional energy was transferred to the heating of the PBL, as seen in Fig. 4.

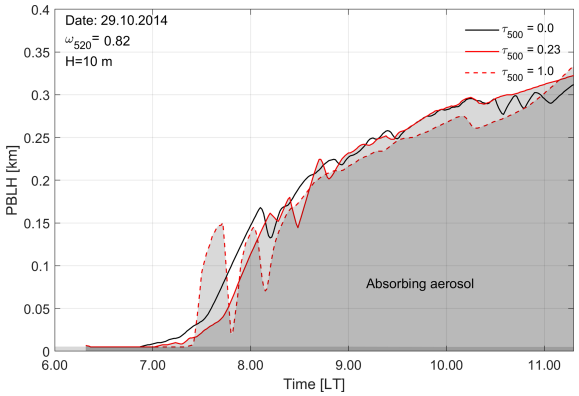

Figure 3. Change in PBLH over time presented on 29 October 2014. The observed PBLH variation is marked with a red line. The gray area indicates a region with a non-zero aerosol concentration. The simulation is compared to the clear-sky case with $\tau_{500} = 0.0$ (black line) and a high-pollution case with $\tau_{500} = 1.0$.

Comparing the simulated PBLH to simulations conducted for clear-sky and high-pollution cases, we observe that the higher the concentration of absorbing aerosol, the greater the delay in the onset of convective mixing. For $\tau_{500} = 1.0$, the delay was ~ 20 min later than for the clear-sky case. The dynamics of convection itself also change. At high concentrations of absorbing aerosol, we observe rapid formation and disappearance of thermals, and the PBL does not stabilize until 09:00 LT.

Secondly, we used EDMF-AERO's unique functionality, enabling us to study one component effect at a time. We compared cases with isolated components of "surface cooling" and "atmospheric heating" (see Sect. 1) to cases with both components turned on and off.

Examining Fig. 4, we see that the simulation with the isolated "surface cooling" component resulted in average potential temperature in PBL $\overline{\theta_{\mathrm{PBL}}} = 282.19$ K and PBLH $=$ 0.27 km. Compared to the control case, this is -0.61 K (-6.3 %) and -0.03 km (-10 %) reduction in potential temperature and PBLH, respectively. For the "atmospheric heating" component we got $\overline{\theta_{\mathrm{PBL}}} = 284.04$ K and PBLH $=$ 0.34 km. Compared to the control case, this is 1.24 K (12.8 %) and 0.04 km (13 %) increase in potential temperature and PBLH, respectively. This suggests that the "atmospheric heating" component has a ~ 2 times stronger influence on the $\overline{\theta_{\mathrm{PBL}}}$ than the "surface cooling". In terms of the influence on PBLH, the API effect components are comparable, resulting in an effectively negligible PBLH change when both components are active.

Finally, we examine the heating rate (HR) profiles (see Fig. 5). As expected, such a high concentration of absorbing aerosol near the surface traps a significant amount of energy, leading to values of HR as high as 50 K d^{-1}. Despite that, the PBLH maintains a constant value of ~ 25 m until 07:30 LT, when it rises sharply and reaches ~ 200 m in just 1 h.

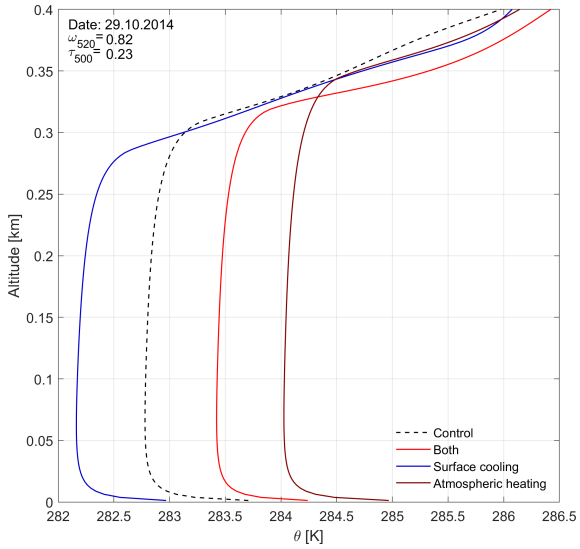

Figure 4. Comparison of EDMF-AERO predictions with individual API component effects turned on or off. The dashed line indicates the control case with both effects turned off. The solid red line marks the case with both component effects turned on. The intermediate cases are marked with blue ("surface cooling") and dark red lines ("atmospheric heating").

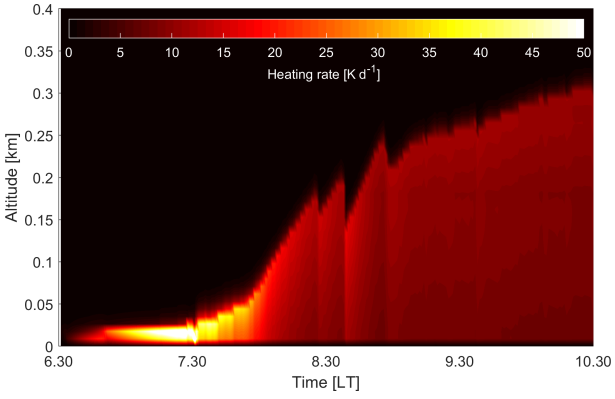

Figure 5. Graph showing the heating rate HR profile over time.

The PBL stabilizes around 09:00 LT, continuing its growth at a slower rate and reaching ~ 300 m around 10:30 LT.

5 Conclusions

Using data collected during the 2014 measurement campaign in the Swider Geophysical Laboratory and a new model, EDMF-AERO, we analyzed the real case of PBL evolution under conditions of high absorbing aerosol concentration.

1. Absorbing aerosol concentration did not significantly affect the PBLH at noon due to component effects "surface cooling" and "atmospheric heating" canceling each other out in these particular atmospheric conditions.

2. The vertical profiles of radiation heating over time were calculated, yielding extreme values of the order of $50\,\mathrm{K\,d^{-1}}$. Most of this energy was transferred into additional heating of the PBL and rapid formation of unstable thermals in the morning.

3. Analysis of isolated aerosol effects showed that the effect component of "atmospheric heating" had over two times stronger influence on average PBL potential temperature at noon than "surface cooling" resulting in effective heating of the PBL.

The findings are a valuable addition to the overall consensus regarding the API effects: the stove and dome. Mainly, it appears that studied conditions (high aerosol optical depths near the surface) invoke a dome effect instead of the expected stove effect. This could be a result of a late October solar path (fall in Poland), low amounts of solar energy reaching the surface, therefore weak convection. This agrees well with the isolated component effect analysis. The influence of "surface cooling" on PBLH cancels out with the "atmospheric heating" part, therefore, effects connected with PBL growth dynamics may be too weak to be detected. This could not be known without the compound effect isolation and further confirms that EDMF-AERO is a useful tool when studying the impact of atmospheric aerosol on the evolution of PBL and API in general.

Data availability. The data are available at:

- Soundings: https://weather.uwyo.edu/upperair/sounding.html (University of Wyoming, 2024)
- PolandAOD Database: https://igf.fuw.edu.pl/~kmark/stacja/PolandAODdata.php (Markowicz, 2025)

Author contributions. GMF: Formal analysis, Methodology, Software, Visualization, Writing. KMM: Conceptualization, Data curation, Supervision.

Competing interests. The contact author has declared that neither of the authors has any competing interests.

Disclaimer. Publisher's note: Copernicus Publications remains neutral with regard to jurisdictional claims made in the text, published maps, institutional affiliations, or any other geographical representation in this paper. While Copernicus Publications makes every effort to include appropriate place names, the final responsibility lies with the authors.

Special issue statement. This article is part of the special issue "EMS Annual Meeting: European Conference for Applied Meteorology and Climatology 2024". It is a result of the EMS Annual Meeting 2024, Barcelona, Spain, 2–6 September 2024. The corresponding presentation was part of session UP1.2: Atmospheric boundary-layer processes, turbulence and land-atmosphere interactions.

Acknowledgements. Authors acknowledge AERONET-Europe/ACTRIS for calibration and maintenance services.

Review statement. This paper was edited by Carlos Román-Cascón and reviewed by Juan Carbone and one anonymous referee.

References

Albrecht, B. A.: Aerosols, Cloud Microphysics, and Fractional Cloudiness, Science, 245, 1227–1230, https://doi.org/10.1126/science.245.4923.1227, 1989.

Barbaro, E., de Arellano, J. V.-G., Ouwersloot, H. G., Schröter, J. S., Donovan, D. P., and Krol, M. C.: Aerosols in the convective boundary layer: Shortwave radiation effects on the coupled land-atmosphere system, J. Geophys. Res.-Atmos., 119, 5845–5863, https://doi.org/10.1002/2013JD021237, 2014.

Brooks, I. M.: Finding Boundary Layer Top: Application of a Wavelet Covariance Transform to Lidar Backscatter Profiles, J. Atmos. Ocean. Tech., 20, 1092–1105, https://doi.org/10.1175/1520-0426(2003)020<1092:FBLTAO>2.0.CO;2, 2003.

Caicedo, V., Rappenglück, B., Lefer, B., Morris, G., Toledo, D., and Delgado, R.: Comparison of aerosol lidar retrieval methods for boundary layer height detection using ceilometer aerosol backscatter data, Atmos. Meas. Tech., 10, 1609–1622, https://doi.org/10.5194/amt-10-1609-2017, 2017.

Chilinski, M., Markowicz, K., and Markowicz, J.: Observation of vertical variability of black carbon concentration in lower troposphere on campaigns in Poland, Atmos. Environ., 137, 155–170, 2016.

Chiliński, M. T., Markowicz, K. M., and Kubicki, M.: UAS as a Support for Atmospheric Aerosols Research: Case Study, Pure Appl. Geophys., 175, 3325–3342, https://doi.org/10.1007/s00024-018-1767-3, 2018.

Ferrero, L., Castelli, M., Ferrini, B. S., Moscatelli, M., Perrone, M. G., Sangiorgi, G., D'Angelo, L., Rovelli, G., Moroni, B., Scardazza, F., Močnik, G., Bolzacchini, E., Petitta, M., and Cappelletti, D.: Impact of black carbon aerosol over Italian basin valleys: high-resolution measurements along vertical profiles, radiative forcing and heating rate, Atmos. Chem. Phys., 14, 9641–9664, https://doi.org/10.5194/acp-14-9641-2014, 2014.

Florczyk, G., Markowicz, K., and Witek, M.: Substantial impacts of absorbing aerosols on PBL evolution in EDMF-AERO modeling framework, Atmos. Environ., 352, 121192, https://doi.org/10.1016/j.atmosenv.2025.121192, 2025.

Fu, Q. and Liou, K.: On the correlated k-distribution method for radiative transfer in nonhomogeneous atmospheres, J. Atmos. Sci., 49, 2139–2156, 1992.

Garcia-Franco, J. and Stremme, W.: Ceilo code documentation of EPR group, CCA UNAM [code], https://eprccaunam.github.io/ceilo/master.html (last access: 1 August 2024), 2018.

García-Franco, J. L., Stremme, W., Bezanilla, A., Ruiz-Angulo, A., and Grutter, M.: Variability of the Mixed-Layer Height Over Mexico 185 City, Bound.-Lay. Meteorol., 167, 493–507, https://doi.org/10.1007/s10546-018-0334-x, 2018.

Grabon, J. S., Davis, K. J., Kiemle, C., and Ehret, G.: Airborne Lidar Observations of the Transition Zone Between the Convective Boundary Layer and Free Atmosphere During the International H2O Project (IHOP) in 2002, Bound.-Lay. Meteorol., 134, 61–83, https://doi.org/10.1007/s10546-009-9431-1, 2010.

Han, J., Witek, M. L., Teixeira, J., Sun, R., Pan, H.-L., Fletcher, J. K., and Bretherton, C. S.: Implementation in the NCEP GFS of a Hybrid Eddy-Diffusivity Mass-Flux (EDMF) Boundary Layer Parameterization with Dissipative Heating and Modified Stable Boundary Layer Mixing, Weather Forecast., 31, 341–352, https://doi.org/10.1175/WAF-D-15-0053.1, 2016.

Huang, X., Wang, Z., and Ding, A.: Impact of Aerosol-PBL Interaction on Haze Pollution: Multiyear Observational Evidences in North China, Geophys. Res. Lett., 45, 8596–8603, https://doi.org/10.1029/2018GL079239, 2018.

Li, Z., Guo, J., Ding, A., Liao, H., Liu, J., Sun, Y., Wang, T., Xue, H., Zhang, H., and Zhu, B.: Aerosol and boundary-layer interactions and impact on air quality, National Science Review, 4, 810–833, https://doi.org/10.1093/nsr/nwx117, 2017.

Lisok, J., Rozwadowska, A., Pedersen, J. G., Markowicz, K. M., Ritter, C., Kaminski, J. W., Struzewska, J., Mazzola, M., Udisti, R., Becagli, S., and Gorecka, I.: Radiative impact of an extreme Arctic biomass-burning event, Atmos. Chem. Phys., 18, 8829–8848, https://doi.org/10.5194/acp-18-8829-2018, 2018.

Luo, H., Dong, L., Chen, Y., Zhao, Y., Zhao, D., Huang, M., Ding, D., Liao, J., Ma, T., Hu, M., and Han, Y.: Interaction between aerosol and thermodynamic stability within the planetary boundary layer during wintertime over the North China Plain: aircraft observation and WRF-Chem simulation, Atmos. Chem. Phys., 22, 2507–2524, https://doi.org/10.5194/acp-22-2507-2022, 2022.

Ma, Y., Ye, J., Xin, J., Zhang, W., Vilà-Guerau de Arellano, J., Wang, S., Zhao, D., Dai, L., Ma, Y., Wu, X., Xia, X., Tang, G., Wang, Y., Shen, P., Lei, Y., and Martin, S. T.: The Stove, Dome, and Umbrella Effects of Atmospheric Aerosol on the Development of the Planetary Boundary Layer in Hazy Regions, Geophys. Res. Lett., 47, e2020GL087373, https://doi.org/10.1029/2020GL087373, 2020.

Ma, Y., Xin, J., Wang, Z., Tian, Y., Wu, L., Tang, G., Zhang, W., de Arellano, J. V.-G., Zhao, D., Jia, D., Ren, Y., Gao, Z., Shen, P., Ye, J., and Martin, S. T.: How do aerosols above the residual layer affect the planetary boundary layer height?, Sci. Total Environ., 814, 151953, https://doi.org/10.1016/j.scitotenv.2021.151953, 2022.

Markowicz, K.: PolandAOD Database, Instytut Geofizyki [data set], https://igf.fuw.edu.pl/~kmark/stacja/PolandAODdata.php, last access: 27 February 2025.

Markowicz, K. M., Stachlewska, I. S., Zawadzka-Manko, O., Wang, D., Kumala, W., Chilinski, M. T., Makuch, P., Markuszewski, P., Rozwadowska, A. K., Petelski, T., Zielinski, T., Posyniak, M., Kaminski, J. W., Szkop, A., Pietruczuk, A., Chojnicki, B. H., Harenda, K. M., Poczta, P., Uscka-Kowalkowska, J., Struzewska, J., Werner, M., Kryza, M., Drzeniecka-Osiadacz, A., Sawinski, T., Remut, A., Mietus, M., Wiejak, K., Markowicz, J., Belegante, L., and Nicolae, D.: A Decade of Poland-AOD Aerosol Research Network Observations, Atmosphere, 12, 1583, https://doi.org/10.3390/atmos12121583, 2021.

Miao, Y., Li, J., Miao, S., Che, H., Wang, Y., Zhang, X., Zhu, R., and Liu, S.: Interaction Between Planetary Boundary Layer and $PM_{2.5}$ Pollution in Megacities in China: a Review, Current Pollution Reports, 5, 261–271, https://doi.org/10.1007/s40726-019-00124-5, 2019.

Nakayama, T., Suzuki, H., Kagamitani, S., Ikeda, Y., Uchiyama, A., and Matsumi, Y.: Characterization of a three wavelength photoacoustic soot spectrometer (PASS-3) and a photoacoustic extinctiometer (PAX), J. Meteorol. Soc. Jpn. Ser. II, 93, 285–308, 2015.

Nash, J., Oakley, T., Voemel, H., and Wei, L.: World meteorological organization instruments and observing methods report no. 107., Tech. rep., WMO, https://www.gruan.org/gruan/editor/documents/wmo/IOM-107_Yangjiang.pdf (last access: 1 August 2024), 2010.

Siebesma, A. and Teixeira, J.: An advection-diffusion scheme for the convective boundary layer: Description and 1D results., in: 14th Symp. on Boundary Layer and Turbulence, Aspen, CO, Amer. Meteor. Soc., 4.16, 2000.

Siebesma, A. P., Soares, P. M. M., and Teixeira, J.: A Combined Eddy-Diffusivity Mass-Flux Approach for the Convective Boundary Layer, J. Atmos. Sci., 64, 1230–1248, https://doi.org/10.1175/JAS3888.1, 2007.

Soares, P. M. M., Miranda, P. M. A., Siebesma, A. P., and Teixeira, J.: An eddy-diffusivity/mass-flux parameterization for dry and shallow cumulus convection, Q. J. Roy. Meteor. Soc., 130, 3365–3384, 2004.

Sokół, P., Stachlewska, I. S., Ungureanu, I., and Stefan, S.: Evaluation of the boundary layer morning transition using the CL-31 ceilometer signals, Acta Geophysica, 62, 367–380, 2014.

Stull, R. B.: An Introduction to Boundary Layer Meteorology, Springer Netherlands, Dordrecht, ISBN 978-94-009-3027-8, https://doi.org/10.1007/978-94-009-3027-8_1, 1988.

Su, T., Li, Z., Li, C., Li, J., Han, W., Shen, C., Tan, W., Wei, J., and Guo, J.: The significant impact of aerosol vertical structure on lower atmosphere stability and its critical role in aerosol–planetary boundary layer (PBL) interactions, Atmos. Chem. Phys., 20, 3713–3724, https://doi.org/10.5194/acp-20-3713-2020, 2020.

Su, T., Li, Z., Zheng, Y., Wu, T., Wu, H., and Guo, J.: Aerosol-boundary layer interaction modulated entrainment process, npj Climate and Atmospheric Science, 5, 64, https://doi.org/10.1038/s41612-022-00283-1, 2022.

Toledo, D., Córdoba-Jabonero, C., and Gil-Ojeda, M.: Cluster Analysis: A New Approach Applied to Lidar Measurements for Atmospheric Boundary Layer Height Estimation, J. Atmos. Ocean. Tech., 31, 422–436, https://doi.org/10.1175/JTECH-D-12-00253.1, 2014.

Twomey, S.: The nuclei of natural cloud formation part II: The supersaturation in natural clouds and the variation of cloud droplet concentration, Geofisica pura e applicata, 43, 243–249, https://doi.org/10.1007/BF01993560, 1959.

University of Wyoming: University of Wyoming Atmospheric Science Radiosonde Archive, University of Wyoming [data set], https://weather.uwyo.edu/upperair/sounding.html, last access: 8 July 2024.